

Solid phase synthesis of anthraquinone peptides and their evaluation as topoisomerase I inhibitors

GREGORY I. GILES and RAM P. SHARMA*

Division of Biochemistry and Molecular Biology, School of Biological Sciences, Bassett Crescent East, University of Southampton, SO16 7PX, UK

Received 20 May 2004; Revised 20 September 2004; Accepted 23 September 2004

Abstract: Anthraquinone peptide derivatives have previously been shown to inhibit the enzyme topoisomerase I (topo I), a pharmaceutical target for the prevention of malignant carcinomas. A highly efficient procedure for the attachment of the anthraquinone moiety to the *N*-terminus of a peptide on a solid support is reported. This methodology provides a convenient method for the synthesis of labelled peptides, with potential applications for chemotherapy, DNA detection and protein purification. As the synthetic strategy utilizes the solid phase, it should also be amenable to the generation of combinatorial libraries. The utility of the method by synthesizing a pool of peptides and assaying for topo I inhibition is demonstrated. Copyright © 2005 European Peptide Society and John Wiley & Sons, Ltd.

Keywords: anthraquinone peptide derivatives; topoisomerase I inhibitors

INTRODUCTION

Intense interest has been focused on the anthraquinone pharmacophore due to its potential utility in cancer chemotherapy. The planar anthraquinone ring system is able to bind DNA by inserting between DNA base pairs, a binding mode termed intercalation [1]. This enables drugs based on the anthraquinone scaffold to interact with DNA metabolizing enzymes. Inhibition of the DNA relaxing enzymes topoisomerase I and II (topo I and II) results in the stabilization of a ternary complex between inhibitor, DNA and enzyme termed the 'cleavable complex' [2]. During the process of cell mitosis it is thought that this complex collides with the replication fork to produce broken strands of DNA, an event that induces the cell to undergo apoptosis (programmed cell death) [3]. Of the drugs in common clinical use for chemotherapy, doxorubicin and mitoxantrone have been shown to form cleavable complexes with topo II and camptothecin and its analogues (Figure 1) with topo I [2,3]. As such, topoisomerase inhibition represents a key therapeutic target in chemotherapy. The clinical dosage of topoisomerase inhibitors is limited by their cardiotoxicity, due to non-specific binding and redox-metabolism of the anthraquinone moiety resulting in the generation of free radical species [4,5]. There is therefore a need to generate increased structural diversity for substituted anthraquinones in order to ameliorate the side effects clinically experienced with this class of drug.

Although there has been extensive work in the synthesis of anthraquinones with *bis*-amine substitutions [6–8] this synthetic route is limited in scope

to simple amines. An alternative approach has been to functionalize the anthraquinone moiety with an aminoalkyl spacer, which functions as a linker upon which a peptide chain can be constructed [9,10]. This methodology allows for greater structural diversity but is hindered by the necessity of the spacer region between the two pharmacophores. Cummings and co-workers have developed a solution phase synthesis of a range of anthraquinones mono-substituted with a range of amino acids and dipeptides [11–13]. Upon biological evaluation some of the compounds were found to inhibit the action of topo I, although they showed no cleavable complex formation with topo II [11–13]. *In vitro* assays showed that the compounds which exhibited topo I inhibition possessed moderate activity against tumour cell lines and one of these compounds, 4-hydroxy-anthraquinone-1-ylTyr ethyl ester showed antitumour activity against HT-29 (colon cancer) and NXOO2 (non small-cell lung cancer) xenografts in mice [11]. As yet few attempts have been made to synthesize these molecules on the solid phase, presumably in part due to the absence of suitable synthetic methodology. This paper reports the first solid phase synthesis of anthraquinone-peptides (Figure 2) with the anthraquinone moiety directly linked to the amino terminus of the peptide. These novel anthraquinone-peptides are further evaluated as topo I inhibitors and relationships obtained between their structure and inhibitory activity.

MATERIALS AND METHODS

Boc amino acids and resins were purchased from Novabiochem Ltd, Nottingham, UK. All other chemicals unless otherwise stated were obtained from Aldrich Chemical Co, Dorset, UK. Dried organic solvents were obtained by storing the

* Correspondence to: Dr Ram P. Sharma, Division of Biochemistry and Molecular Biology, School of Biological Sciences, Bassett Crescent East, University of Southampton, SO16 7PX, UK; e-mail: rps2@soton.ac.uk

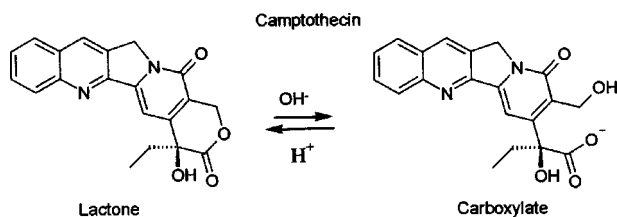


Figure 1 Structure of camptothecin (CPT), a known topo I inhibitor, in ring closed (lactone) and ring opened (carboxylate) forms.

commercially available solvents over activated 4Å molecular sieves. Organic solutions were dried over anhydrous sodium sulphate. All reactions were carried out under a positive nitrogen pressure unless otherwise stated. Agarose for gel electrophoresis was supplied by Pharmacia AB, Uppsala, Sweden. Topo I enzyme was purchased from TopoGEN Inc. Ohio, USA. Chromatography columns were packed using 25 g of silica gel 60.

NMR spectra were recorded on a Bruker 300 MHz instrument. Mass spectra were recorded on a Micromass VG Quatro II mass spectrometer operating in electrospray mode. UV spectra were recorded on a Hitachi U-2000 spectrophotometer. RP-HPLC procedures were performed using a Gilson 715 Instruments apparatus equipped with two slave 306 pumps. Solvent A consisted of TFA/H₂O (0.1% v/v), solvent B of TFA/MeCN (0.1% v/v). Both solvents were filtered through a 45 µm pore filter prior to use. Absorption readings were taken on an Applied Biosystems 759A absorbance detector. Gel photographs were recorded by an Epson GT-8000 scanner. Densitometric analysis was performed using the Phoretix v.5.01 software package, Non-Linear Dynamics Ltd, Newcastle.

Analytical and Preparative RP-HPLC

For analytical RP-HPLC, the peptide sample (1 mg) was placed in an Eppendorf (1 ml) and dissolved in MeCN/H₂O (200 µl, 1 : 1 v/v.) The sample was centrifuged and an aliquot (10 µl) injected onto a C-18 analytical column (Vydac). The sample was eluted by a gradient of 0 to 80% solvent B over a period of 20 min with a flow rate of 1 ml/min monitoring at 216 nm. For preparative RP-HPLC the crude peptide (15 mg) was dissolved in DMF (20 ml). Solvent A (100 ml) was added and the solvent was filtered through a 45 µm pore filter. The filtrate was

pumped onto a C-18 preparative column (Spherisorb) via a 3-way tap and syringe in the inlet tube to the slave 306 pump for solvent A. The peptide was eluted by a gradient running from 0 to 100% B in 30 min at a flow rate of 10 ml/min monitoring at 230 nm. The elutant was lyophilized overnight. The product was examined by analytical RP-HPLC and the procedure repeated until greater than 99% pure (typically two or three runs). The final product was then dried in a desiccator over phosphorous pentoxide.

Solid Phase Synthesis of Anthraquinone Peptides

The reaction was performed on a 0.25 mmol scale using the Boc strategy. The initial loading reaction was performed by the *in situ* formation of the active ester of the Boc amino acid with subsequent attachment to the hydroxyl group with 3 equivalents each (relative to the amount of free amine on the resin) of the Boc protected amino acid, DCC, HOBT and 1 equivalent of DMAP in DCM (10 ml). The reaction vessel was shaken for 2 h and then the resin was washed with DCM (3 × 10 ml) and DMF (3 × 10 ml). The Boc group was removed by treating the resin with TFA/DCM (10 ml, 1 : 1 v/v) for 30 min. The resin was then washed with DCM (10 ml, 3 × 5 min) and a quantitative ninhydrin assay was performed to determine the substitution.

For each subsequent coupling step 3 equivalents each of Boc amino acid, BOP, HOBT and 9 equivalents of DIPEA in DCM (10 ml) were used and the reaction was carried out for 40 min. The resin was washed with DMF (3 × 10 ml) and DCM (3 × 10 ml) and subjected to the ninhydrin assay. The procedure was repeated until the ninhydrin assay gave a negative result. The Boc group was then removed and the resin was washed as usual with DCM (10 ml, 3 × 5 min). The cycle of coupling and deprotection was repeated until the desired sequence of amino acids was assembled. A final deprotection step was performed and the resulting TFA salt neutralized by washing with a DIPEA/DMF solvent (10 ml, 2% v/v, 2 × 10 min) to obtain a free amino terminus. The resin was washed with DMF (3 × 10 ml), DCM (3 × 10 ml), diethyl ether (3 × 10 ml) and dried under reduced pressure.

Condensation of Leuco-quinizarin and Amino-terminus of the Peptide

The dried resin was transferred to a 2-necked round bottom flask (250 ml) equipped with stirrer bar and condenser.

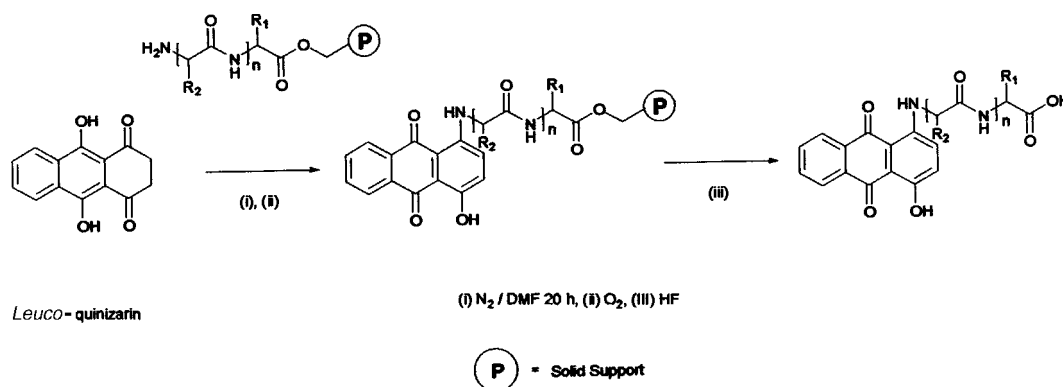


Figure 2 Synthetic route for the solid phase synthesis of mono substituted anthraquinone peptides.

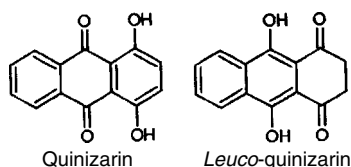


Figure 3 Chemical structures of quinizarin and leuco-quinizarin.

Leuco-quinizarin (Figure 3b) was prepared from quinizarin (Figure 3a) by the procedure of Greenhalgh and Hughes [14] and purified by column chromatography before each condensation reaction. Leuco-quinizarin (180 mg, 0.75 mmol, 3 eq.) was then added to the round bottom flask containing the resin. Dry DMF (20 ml) was added and the flask and condenser was flushed with nitrogen and sealed with a rubber septum. A positive pressure of nitrogen was maintained and the apparatus lowered into an oil bath pre-heated to 120 °C and left stirring overnight. Acetone (200 ml) was added to the warm reaction mixture with stirring and oxygen was gently bubbled through for 2 h. The resin was then filtered and washed with DMF (100 ml), acetone (100 ml), DCM (100 ml) and then with diethyl ether (3 × 20 ml). The resin was then dried under reduced pressure.

High HF Cleavage

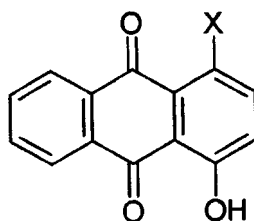
The resin was placed in a Teflon vessel and a *p*-creosol scavenger (50 mg) was added. The vessel was cooled in liquid

nitrogen and evacuated. Anhydrous HF (15 ml) was distilled into the vessel and the mixture was stirred at 0 °C for 1 h. The HF was removed by a stream of nitrogen gas. The resin was first washed with diethyl ether (3 × 20 ml), treated with TFA/DCM (50 ml, 1:1 v/v) and the filtrate was concentrated under reduced pressure. Cold diethyl ether (20 ml) was added and the precipitate filtered and washed with diethyl ether (3 × 20 ml) to give crude product, which was purified by RP-HPLC and characterized by ESMS. All new compounds (Table 1) reported in this paper gave satisfactory analytical data.

4-Hydroxy-anthraquinone-1-ylGlyGly 1. UV-Vis (DMF) λ (log ϵ) 555 (3.97) 594 (3.92) nm, $^1\text{H NMR}$ (300 MHz, $(\text{CD}_3)_2\text{SO}$) δ , 4.18 (d, $J = 4.8$ Hz, 2H, glycylic CH_2) 3.84 (d, $J = 5.5$ Hz, 2H, glycylic CH_2) 7.27 (d, $J = 9.6$ Hz, 1H, anthraquinone CH_2) 7.37 (d, $J = 9.6$ Hz, 1H, anthraquinone CH_3) 7.80–8.05 (m, 2H, anthraquinone $\text{CH}_{6,7}$) 8.20–8.35 (m, 2H, anthraquinone $\text{CH}_{5,8}$) 8.45–8.55 (m, 1H, NHCO) 10.35–10.45 (m, 1H, anthraquinone NH) 12.45–12.80 (s br, 1H, CO_2H) 13.5 (s, 1H, anthraquinone OH).

4-Hydroxy-anthraquinone-1-ylGly β Ala 2. UV-Vis (DMF) λ (log ϵ) 554 (3.97) 591 (3.85) nm, $^1\text{H NMR}$ (300 MHz, $(\text{CD}_3)_2\text{SO}$) δ 2.42 (t, $J = 6.8$ Hz, 2H, β alanyl CH_2) 3.2–3.5 (β alanyl CH_2 , obscured by water) 4.06–4.14 (m, 2H, glycylic CH_2) 7.25 (d, $J = 9.6$ Hz, 1H, anthraquinone CH_2) 7.39 (d, $J = 9.6$ Hz, 1H, anthraquinone CH_3) 7.85–8.01 (m, 2H, anthraquinone $\text{CH}_{6,7}$) 8.20–8.31 (m, 3H, anthraquinone

Table 1 Structure, RP-HPLC Retention Time and Mass Spectra for Anthraquinone Peptides Studied. N/A: Not applicable



Compound	X	RP-HPLC Retention time/min	ESMS m/z
1	Gly-Gly-OH	17.2	354 [M - H] ⁻
2	Gly- β Ala-OH	18.1	367 [M - H] ⁻
3	β Ala-Gly-NH ₂	17.4	368 [M + H] ⁺
4	L-Ala-Gly-NH ₂	12.3	368 [M + H] ⁺
5	L-Ser-Gly-NH ₂	17.8	383 [M - H] ⁻
6	L-Tyr-Gly-NH ₂	19.6	460 [M + H] ⁺
7	L-Tyr-Gly-OH	18.7	459 [M - H] ⁻
8	L-Tyr-L-Ala-OH	19.7	473 [M - H] ⁻
9	L-Tyr- β Ala-OH	19.2	473 [M - H] ⁻
10	Gly-L-Tyr-OH	19.0	459 [M - H] ⁻
11	L-Phe-OH	N/A	443 [M - H] ⁻
12	L-Tyr-OH	N/A	403 [M - H] ⁻
13	Phe (NO ₂)	N/A	387 [M - H] ⁻
14	Gly-Gly-L-Lys-L-Arg-L-Ala-L-Arg-L-Glu-L-Asn-L-Thr-L-Glu-L-Ala-Gly-NH ₂	14.4	446 [M + 3H] ³⁺
15	Gly-L-Ser-L-Ala-Gly-NH ₂	17.3	512 [M + H] ⁺

CH5,8 & CONH) 10.33–10.44 (m, 1H, NH) 13.57 (s, 1H, anthraquinone OH).

4-Hydroxy-anthraquinone-1-yl β AlaGly-NH₂ 3. UV-Vis (DMF) λ (log ϵ) 554 (3.97) 591 (3.84) nm, ¹H NMR (300 MHz, (CD₃)₂SO) δ , 2.54 (t, J = 6.9 Hz, 2H, β alanyl CH₂) 3.20–3.50 (β alanyl CH₂, obscured by water) 3.60–3.70 (m, 2H, glyceryl CH₂) 7.02–7.08 (s, 1H, CONH₂ Ha) 7.30 (s, 1H, CONH₂ Hb) 7.34 (d, J = 9.6 Hz, 1H, anthraquinone CH₂) 7.53 (d, J = 9.6 Hz, 1H, anthraquinone CH₃) 7.76–7.94 (m, 2H, anthraquinone CH_{6,7}) 8.16–8.27 (m, 3H, anthraquinone CH_{5,8} & CONH) 10.21–10.29 (m, 1H, anthraquinone NH) 13.61 (s, 1H, anthraquinone OH).

4-Hydroxy-anthraquinone-1-ylAlaGly-NH₂ 4. UV-Vis (DMF) λ (log ϵ) 555 (3.97) 598 (3.84) nm, ¹H NMR (300 MHz, (CD₃)₂SO) δ , 1.44 (d, J = 6.6 Hz, 3H, alanyl CH₃) 3.65–3.75 (m, 2H, glyceryl CH₂) 4.45–4.55 (t, J = 7.0 Hz, 1H, CH) 7.08 (s, 1H, CONH₂ Ha) 7.33 (d, J = 9.6 Hz, 1H, anthraquinone CH₂) 7.36 (s, 1H, CONH₂ Hb) 7.39 (d, J = 9.6 Hz, 1H, anthraquinone CH₃) 7.83–8.01 (m, 2H, anthraquinone CH_{6,7}) 8.21–8.39 (m, 3H, anthraquinone CH_{5,8} & CONH) 10.45 (1H, anthraquinone NH) 13.57 (s, 1H, anthraquinone OH).

4-Hydroxy-anthraquinone-1-ylSerGly-NH₂ 5. UV-Vis (DMF) λ (log ϵ) 553 (3.96) 595 (3.85) nm, ¹H NMR (300 MHz, (CD₃)₂SO) δ , 3.60–3.90 (m, 4H, seryl CH₂OH & glyceryl CH₂) 4.43–4.51 (m, 1H, seryl α CH) 7.15 (s, 1H, CONH₂ Ha) 7.31 (s, 1H, CONH₂ Hb) 7.36 (d, J = 9.6 Hz, 1H, anthraquinone CH₂) 7.4 (d, J = 9.6 Hz, 1H, anthraquinone CH₃) 7.86–8.00 (m, 2H, anthraquinone CH_{6,7}) 8.23–8.35 (m, 3H, anthraquinone CH_{5,8} & CONH) 10.52 (1H, anthraquinone NH) 13.58 (s, 1H, anthraquinone OH).

4-Hydroxy-anthraquinone-1-ylTyrGly-NH₂ 6. UV-Vis (DMF) λ (log ϵ) 555 (3.97) 589 (3.94) nm, ¹H NMR (500 MHz, CF₃COOD) δ , 3.27–3.35 (m, 2H, tyrosyl β CH₂) 3.86–4.09 (m, 2H, glyceryl CH₂) 4.69–4.77 (m, 1H, tyrosyl α CH) 6.71 (d, J = 8.6 Hz, 2H, tyrosyl ar. CH) 6.97 (d, J = 8.6 Hz, 2H, tyrosyl ar. CH) 7.34 (d, J = 9.6 Hz, 1H, anthraquinone CH₂) 7.62, (d, J = 9.6 Hz, 1H, anthraquinone CH₃) 7.75–7.81 (m, 2H, anthraquinone CH_{6,7}) 8.15–8.23 (m, 3H, anthraquinone CH_{5,8} & CONH) 10.64 (1H, anthraquinone NH) 13.57 (s, 1H, anthraquinone OH).

4-Hydroxy-anthraquinone-1-ylTyrGly 7. UV-Vis (DMF) λ (log ϵ) 280 (3.92), 555 (3.90) 593 (3.88) nm, ¹H NMR (300 MHz, (CD₃)₂SO) δ , 2.85–3.20 (m, 2H, tyrosyl β CH₂) 3.78 (2H, glyceryl CH₂) 4.54–4.67 (m, 1H, tyrosyl α CH) 6.64 (d, J = 8.5 Hz, 2H, tyrosyl ar. CH) 7.10 (d, J = 8.5 Hz, 2H, tyrosyl ar. CH) 7.23 (d, J = 9.6 Hz, 1H, anthraquinone CH₂) 7.28 (d, J = 9.6 Hz, 1H, anthraquinone CH₃) 7.83–7.99 (m, 2H, anthraquinone CH_{6,7}) 8.21–8.39 (m, 3H, anthraquinone CH_{5,8} & CONH) 9.25 (s, 1H, tyrosyl OH) 10.45 (1H, anthraquinone NH) 13.5 (s, 1H, anthraquinone OH).

4-Hydroxy-anthraquinone-1-ylTyrAla 8. UV-Vis (DMF) λ (log ϵ) 556 (3.90), 594 (3.85) nm, ¹H NMR (300 MHz, (CD₃)₂SO) δ , 1.29 ((d, J = 7.4 Hz, 3H, alanyl CH₃) 2.79–2.95 (m, 1H, tyrosyl β CH₂ Ha) 3.05–3.20 (m, 1H, partially obscured by water, tyrosyl β CH₂ Hb) 4.18–4.30 (m, 1H, alanyl α CH) 4.56–4.67 (m, 1H, tyrosyl α CH) 6.62 (d J = 8.5 Hz, 2H, tyrosyl ar. CH) 7.08 (d J = 8.5 Hz, 2H, tyrosyl ar. CH) 7.16 (d J = 9.6 Hz, 1H, anthraquinone CH₂) 7.29 (d J = 9.6 Hz, 1H, anthraquinone CH₃) 7.82–7.99 (m, 2H, anthraquinone

CH_{6,7}) 8.20–8.41 (m, 3H, anthraquinone CH_{5,8} & CONH) 9.23 (s, 1H, tyrosyl OH) 10.48 (1H, anthraquinone NH) 13.60 (s, 1H, anthraquinone OH).

4-Hydroxy-anthraquinone-1-ylTyr β Ala 9. UV-Vis (DMF) λ (log ϵ) 557 (3.83), 594 (3.82) nm, ¹H NMR (300 MHz, (CD₃)₂SO) δ , 2.29–2.40 (m, 2H, β alanyl CH₂) 2.84–3.09 (m, 2H, tyrosyl β CH₂) 3.20–3.34 (m, 2H, partially obscured by water, β alanyl CH₂) 4.46–4.57 (m, 1H, tyrosyl α CH) 6.64 (d J = 8.5 Hz, 2H, tyrosyl ar. CH) 7.07 (d J = 8.5 Hz, 2H, tyrosyl ar. CH) 7.19 (d J = 9.6 Hz, 1H, anthraquinone CH₂) 7.28 (d J = 9.6 Hz, 1H, anthraquinone CH₃) 7.81–7.99 (m, 2H, anthraquinone CH_{6,7}) 8.18–8.34 (m, 3H, anthraquinone CH_{5,8} & CONH) 9.24 (s, 1H, tyrosyl OH) 10.45 (1H, anthraquinone NH) 12.25 (s br, 1H, CO₂H) 13.54 (s, 1H, anthraquinone OH).

4-Hydroxy-anthraquinone-1-ylGlyTyr 10. UV-Vis (DMF) λ (log ϵ) 554 (3.91) 589 (3.84) nm, ¹H NMR (300 MHz, (CD₃)₂SO) δ , 2.73–2.82 (m, 1H, tyrosyl β CH₂ Ha) 2.96–3.02 (m, 1H, tyrosyl β CH₂ Hb) 4.04–4.11 (m, 2H, glyceryl CH₂) 4.43–4.46 (m, 1H, tyrosyl α CH) 6.66 (d, J = 8.5 Hz, 2H, tyrosyl ar. H) 7.02 (d, J = 8.5 Hz, 2H, tyrosyl ar. H) 7.06 (d, J = 9.6 Hz, 1H, anthraquinone CH₂) 7.30 (d, J = 9.6 Hz, 1H, anthraquinone CH₃) 7.80–7.95 (m, 2H, anthraquinone CH_{6,7}) 8.19–8.35 (m, 3H, anthraquinone CH_{5,8} & CONH) 9.26 (s, 1H, tyrosyl OH) 10.4 (1H, anthraquinone NH) 13.55 (s, 1H, anthraquinone OH).

4-Hydroxy-anthraquinone-1-ylPhe 11. TLC (5% v/v MeOH/CHCl₃) R_f 0.15, UV-Vis (DMF) λ (log ϵ) 556 (3.75) 597 (3.65) nm, ¹H NMR (300 MHz, CD₃CN) δ , 2.96–3.20 (m, 2H, partially obscured by water, Phe β CH₂) 4.45–4.60 (m, 1H, Phe α CH) 7.05–7.40 (m, 7H, Phe ar.H. and anthraquinone CH_{2,3}) 7.80–7.93 (m, 2H, anthraquinone CH_{6,7}) 8.21–8.32 (m, 2H, anthraquinone CH_{5,8}) 10.60 (1H, anthraquinone NH) 13.69 (s, 1H, anthraquinone OH).

4-Hydroxy-anthraquinone-1-ylTyr 12. TLC (30% v/v MeOH/CHCl₃) R_f 0.42, UV-Vis (DMF) λ (log ϵ) 560 (3.84) 598 (3.72) nm, ¹H NMR (300 MHz, CD₃CN) δ , 3.05–3.30 (m, 2H, partially obscured by water, tyrosyl β CH₂) 4.65–4.77 (m, 1H, tyrosyl α CH) 6.68 (d J = 8.4 Hz, 2H, tyrosyl ar. H) 7.07 (d J = 8.4 Hz, 2H, tyrosyl ar. H) 7.16 (d, J = 9.6 Hz, 1H, anthraquinone CH₂) 7.30 (d, J = 9.6 Hz, 1H, anthraquinone CH₃) 7.73–7.95 (m, 2H, anthraquinone CH_{6,7}) 8.23–8.38 (m, 2H, anthraquinone CH_{5,8}) 10.41 (1H, anthraquinone NH) 13.55 (s, 1H, anthraquinone OH).

4-Hydroxy-anthraquinone-1-ylPhe(NO₂) 13. TLC (20% v/v MeOH/CHCl₃) R_f 0.38, UV-Vis (DMF) λ (log ϵ) 583 (3.78) 622 (3.72) nm, ¹H NMR (300 MHz, CD₃CN) δ , 3.20–3.60 (m, 2H, obscured by water, Phe β CH₂) 4.46–4.58 (m, 1H, Phe α CH) 7.18 (d, J = 9.6 Hz, 1H, anthraquinone CH₂) 7.26 (d, J = 9.6 Hz, 1H, anthraquinone CH₃) 7.36–7.53 (m, 2H, Phe ar. H) 7.68–7.96 (m, 2H, Phe ar. H) 7.99–8.08 (m, 2H, anthraquinone CH_{6,7}) 8.18–8.29 (m, 2H, anthraquinone CH_{5,8}) 10.53 (1H, anthraquinone NH) 13.71 (s, 1H, anthraquinone OH).

4-Hydroxy-anthraquinone-1-ylGly-Gly-Lys-Arg-Ala-Arg-Glu-Asn-Thr-Glu-Ala-Gly-NH₂ 14. UV-Vis (H₂O) λ (log ϵ) 317 (3.43) 544 (3.49) 577 (3.40) nm.

4-Hydroxy-anthraquinone-1-ylGly-Ser-Ala-Gly-NH₂ 15. UV-Vis (DMF) λ (log ϵ) 554 (3.86) 584 (3.80) nm, ¹H NMR (300 MHz,

(CD₃)₂SO) δ 1.26 (d J = 6.9 Hz, 3H, alanyl CH₃) 3.57–3.68 (m, 4H, glycylic CH₂ & seryl β CH₂OH) 4.16–4.35 (m, 3H, alanyl α CH & glycylic CH₂) 4.38–4.47 (m, 1H, seryl α CH) 5.14–5.18 (m, 1H, seryl OH) 7.11 (s, 1H, CONH₂ Ha) 7.16 (s, 1H, CONH₂ Hb) 7.29 (d J = 9.6 Hz, 1H, anthraquinone CH₂) 7.39 (d J = 9.6 Hz, 1H, anthraquinone CH₃) 7.83–8.01 (m, 2H, anthraquinone CH_{6,7}) 8.06 (1H, CONH) 8.21–8.42 (m, 4H, anthraquinone CH_{5,8} & 2 CONH) 10.38–10.49 (m, 1H, anthraquinone NH) 13.57 (s, 1H, anthraquinone OH).

Topoisomerase I Inhibition Assay

The linking number of DNA is a mathematical relationship for quantifying the amount of supercoiling of the DNA polymer. For constrained sections of DNA it has been shown that the number of times each polynucleotide chain crosses over the other (twisting number) and the number of times each double stranded section crosses over itself (writhing number) are related [15]. Physical manipulation of double stranded DNA can result in different topomers, converting T to W or vice versa, but cannot change the overall number of crosses. This number of crosses is therefore a more accurate description of the supercoiled state of the DNA than either the T or W number alone and is represented by the linking number L (where $L = T + W$) [15]. In order to metabolize DNA it is necessary to unwind it from its supercoiled storage topomer. As the DNA is constrained between nucleosomes nature has evolved the topoisomerase enzymes as a means of changing the linking number of sections of DNA and so removing supercoils. Topo I changes L in integer steps of one while topo II changes L in steps of 2 [16]. In the case of topo I the enzyme accomplishes this by transiently creating a single stranded nick in the phosphodiester backbone of one DNA strand, with the Tyr723 residue of the enzyme forming a covalent bond on the 3' side of the break [17]. In effect this abolishes the linking number constraint, allowing the DNA to freely rotate about the remaining phosphodiester bond, reducing supercoils without increasing the number of helical repeats. The enzyme then re-ligates the backbone, regenerating the DNA polymer with a lower linking number [17]. Topo I cleavable complex inhibitors interfere with this event by stabilizing the reaction intermediate at the point in the mechanism when the enzyme has cross-linked to the DNA and severed one phosphodiester bond, preventing further progression in the enzymatic cycle and accumulating nicked DNA.

In the presence of ethidium bromide, agarose gel electrophoresis allows resolution of nicked DNA (form II) from covalently closed circular DNA (form I). Ethidium bromide acts as an intercalator, inserting into the DNA helix and introducing writhes (increasing W) as the DNA unwinds (reducing T) to allow access to the intercalator. Both supercoiled (I_S) and relaxed (I_R) DNA therefore migrate to the same position on an ethidium bromide gel. Nicked DNA, due to its freedom to rotate about the single phosphodiester bond, has no linking constraint and hence shows no increase in writhes upon drug intercalation. Covalently closed plasmids will therefore migrate to approximately the same position on the gel, regardless of whether they were initially relaxed or supercoiled, whereas nicked DNA migrates separately. As such, the shift in the equilibrium position between nicked and covalently closed DNA upon formation of the cleavable complex can be measured by gel electrophoresis. The efficacy of topo I inhibitors

is therefore established by monitoring the amount of nicked DNA produced during the course of an *in vitro* DNA relaxation reaction [1].

Media, pipette tips, stock solutions, distilled water and centrifuge tubes were sterilized by autoclaving at 120 °C and 15 psi for 20 min. Chemicals and proteins were sterilized by filter sterilization where appropriate. Topo I was diluted into the reaction buffer supplied (10 X: 100 mM Tris-Cl pH 7.9, 10 mM EDTA, 1.5 M NaCl, 1% BSA, 1 mM spermidine, 50% glycerol) so that the final concentration of enzyme was 0.5 U/ μ l and stored at –70 °C before use. For the topo I relaxation buffer Tris (1.21 g, 10 mmol), KCl (3.73 g, 50 mmol) and MgCl₂ (1.02 g, 5 mmol) were dissolved in water (75 ml) and the pH was adjusted to 7.5 with concentrated HCl. 0.5 M EDTA (200 μ l, pH 8.0) and BSA (15 mg) were added with stirring and the volume made up to 100 ml. For the agarose gel buffer Tris (108 g, 0.89 mole), boric acid (55 g, 0.89 mole) and 0.5 M EDTA (40 ml, pH 8.0) were diluted with water (2 l) to make a Tris-borate-EDTA (TBE) buffer. This solution was diluted five-fold before being used for electrophoresis. For the topo I stop buffer sucrose (50 g), 0.5 M EDTA (10 ml, pH 8.0) bromophenol blue (100 mg) and SDS (200 μ l, 5% w/v) were dissolved in water (100 ml).

Anthraquinone peptides were dissolved in DMSO at a concentration of 1 mg/ml and diluted to the final assay concentration (125 μ M) in buffer. Plasmid DNA (0.5 μ g) was incubated with relaxation buffer (4.50 μ l), topo I enzyme (10.0 μ l, 5 U) and the drug solution (2.25 μ l) and diluted with water (to 45 μ l). The solution was then incubated at 37 °C for 30 min. A pre-warmed solution of proteinase K/SDS (5.0 μ l, 5 mg/ml proteinase K and 5% w/v SDS) was then added and the mixture incubated for a further 30 min. The reaction was terminated by the addition of stop buffer (5.0 μ l) and an aliquot (20.0 μ l) of the reaction mixture was run on an agarose gel in TBE buffer containing ethidium bromide (1 μ g/ml) at 70 V for 100 min. The agarose gel was then washed with water (3 \times 15 min). The DNA was visualized under a transilluminator and the gel photograph recorded for densitometric analysis. In control experiments with neither enzyme nor inhibitor low background levels of nicked DNA were observed, which were then subtracted from the initial values, leaving a corrected ratio which represents the change in the level of nicked DNA upon addition of the inhibitor. For comparison between compounds, the difference in cleavable complex formation was expressed as a percentage of the amount of cleavable complex formed by compound **12** (125 μ M), the most effective inhibitor. CPT (100 nM) was evaluated as a reference compound. Experiments were repeated three times and the values are expressed as the mean of these experiments (Figure 4).

RESULTS AND DISCUSSION

Peptides with an amide or carboxylic acid at the C-terminus were synthesized manually on the solid phase using standard peptide synthesis protocols. Following the final deprotection step the free amino terminus was linked to *leuco*-quinizarin (presumably via formation of the Schiff's base although this putative reaction intermediate was never isolated due to spontaneous oxidation) to form the anthraquinone peptide on the

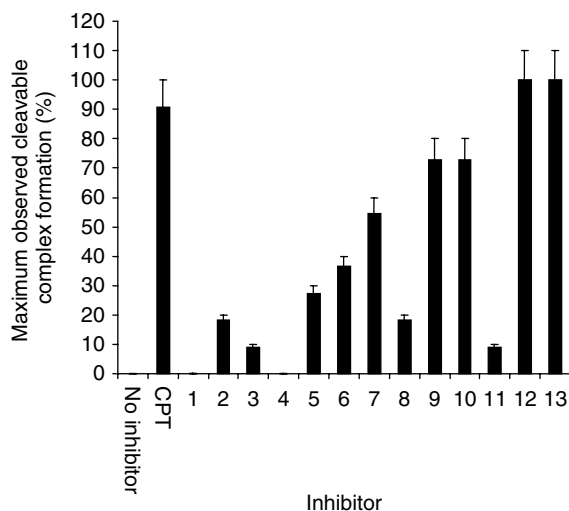


Figure 4 Effect of anthraquinone peptides on Topo I cleavable complex formation. Cleavage reactions were performed using the method described by Hsiang *et al.* [11] with modified reaction conditions (see methods section). The amount of cleavable complex formed for each inhibitor was expressed as a percentage of the amount formed by **12**, the most active inhibitor. The inhibitory activity of anthraquinone peptides **1–13** (125 μM) was compared with that of CPT (100 nM). Experiments were repeated ($n = 3$) and error bars (SD) applied.

solid support. HF cleavage resulted in liberation of the target compound in high yield (Figure 2). For anthraquinone peptides with a requirement for a free carboxylic acid at the C-terminus the synthesis was conducted on Merrifield's hydroxymethyl resin while the peptides requiring an amide group at the C-terminus the MBHA resin was utilized. This method of synthesizing anthraquinone peptides is therefore applicable to a number of solid phase protocols.

The conditions required to attach the anthraquinone group to the peptide chain are not typical of peptide synthesis. The successful synthesis of compounds **14** and **15** indicates that the methodology is applicable to the synthesis of anthraquinone peptides with longer sequences than the dipeptides presented in this paper. The compounds **14** and **15** were not used in biological studies.

A selected range of compounds based on known topoisomerase inhibitors [11] (Table 1) were synthesized and evaluated for their topo I inhibitory activity (Figure 4). Analysis of the experimental inhibition data supports a consistent structure-activity relationship for the anthraquinone peptides as topo I inhibitors that may lead to the future development of more active analogues. From the pool of compounds synthesized, the two phenylalanine derivatives para substituted with either a hydroxy or a nitro group (**12** and **13**) have emerged as the most active compounds in the topo I inhibition assay. Both were more active than the CPT standard, although at a much greater concentration (125 μM compared with 100 nM). The

dipeptide tyrosine analogues **6–10** showed reduced activity when compared with **12**, suggesting that a single amino acid is the optimum requirement in the anthraquinone side chain. For the dipeptides, conversion of the carboxylic acid to an amide for **6** as opposed to **7** resulted in a decrease in activity, indicating a preference for the carboxyl group. In contrast, the Tyr and 4-nitro Phe derivatives **12** and **13** were equally active, showing more tolerance for the aromatic substituent. A group with hydrogen bonding capabilities was, however, important, as the Phe derivative **11** showed a large decrease in cleavable complex formation when compared with either **12** or **13**. Similarly the Ser derivative **5** also showed similar activity to the equivalent Tyr analogue **6**, whereas the Ala analogue **4** showed no activity. The presence of a hydrophilic group on the first amino acid attached to the anthraquinone ring system was therefore extremely important. Confirming this conclusion, the alkyl chain Ala, Gly and β Ala derivatives **1–5** showed little to no activity. However, increasing the length of chain resulted in a slight gain in activity as both peptides **2** and **3** (with β Ala residues extending the peptide chain by a methylene unit) showed enhanced cleavable complex formation.

The ability of the most active anthraquinone peptides to stabilize cleavable complex formation in an analogous manner to CPT prompts a structural comparison between the two classes of compound. In aqueous solution CPT is in dynamic equilibrium between the lactone and carboxylate species due to hydrolytic ring opening, with the lactone predominating at low pH and the carboxylate under basic conditions (Figure 1). The α hydroxy group adjacent to the lactone functionality is thought to stabilize the tetrahedral transition state and so increase the rate of hydrolysis, rendering the lactone ring more reactive than is generally the case with cyclic esters [18]. At pH 7.5 the equilibrium position results in the carboxylate as the predominant species [18]. Additionally synthetic derivatives resistant to hydrolysis due either to the removal of the α hydroxy group or to modifications to the lactone show a loss of topo I inhibitory activity [16]. It is therefore reasonable to compare the most active anthraquinone peptides with the carboxylate form of CPT. Such a comparison of **12** and **13** to CPT reveals several similarities. Both possess extensively conjugated aromatic ring systems allowing intercalation binding with DNA. Additionally both compounds possess a carboxylic acid and either an alcohol or nitro group, giving possibilities for hydrogen bonding interactions with the topo I enzyme to stabilize the cleavable complex. The identification of such structure-activity relationships is predicted to be of use in the future design of topo I inhibitors.

Although this paper has primarily focused on the synthesis of anthraquinone peptides for their potential use in chemotherapy, the solid phase methodology

is widely applicable for alternative applications. The anthraquinone ring system functions as an intense chromophore ($\lambda = 550 \text{ E}^{\text{max}} = 8000 \text{ M}^{-1} \text{ cm}^{-1}$) allowing the detection of peptides by UV-Vis spectroscopy. As such it provides an attractive choice for labelling peptides, either at the *N*-terminus or on the amino groups of lysine or ornithine. The facile synthesis of anthraquinone labelled peptides allows a range of biochemical applications to be explored. Dye-ligand affinity systems have already been used for protein purification [19] and labelled peptides as biochemical probes for DNA detection [20]. It is therefore anticipated that anthraquinone peptides will find diverse biological applications.

Acknowledgements

The authors are grateful to Drs. Jeff Cummings and Gary Boyd at the medical oncology unit of Edinburgh Western General Hospital for the help and the use of their facilities. We thank Imperial Cancer Research Fund and the University of Southampton for providing with financial support for the project and the Division of Biochemistry and Molecular Biology for the use of ES-MS facilities.

REFERENCES

- Hsiang Y-H, Hertzberg R, Hecht S, Liu L. Camptothecin induces protein-linked breaks via mammalian topoisomerase I. *J. Biol. Chem.* 1985; **260**: 14 873–14 878.
- Myers CE, Mimnaugh EG, Sinha BK. Chapter XIV. Biochemical mechanisms of tumour cell kill by the anthracyclines. In *Anthracycline and Anthracenedione Based Anticancer Agents*, Lown J. (ed.). Elsevier Science: Amsterdam, 1988; 528–556.
- Hsiang Y-H, Liu L. Identification of mammalian DNA topoisomerase I as an intracellular target of the anticancer drug camptothecin. *Cancer Res.* 1988; **48**: 1722–1726.
- Garnier-Suillerut A. Chapter IV. Metal anthracycline and anthracenedione based complexes as a new class of anticancer agent. In *Anthracycline and Anthracenedione Based Anticancer Agents*, Lown J (ed.). Elsevier Science: Amsterdam, 1988; 130–157.
- Muller I, Jenner A, Bruchelt G, Niethamer D, Halliwell B. Effect of concentration on the cytotoxic mechanism of doxorubicin-apoptosis and oxidative DNA damage. *Biochem. Biophys. Res. Commun.* 1997; **230**: 254–257.
- Murdock K, Child R, Fabio P, Angier R, Wallace R, Durr F, Citarella R. Antitumour agents 1. 1,4-bis[(aminoalkyl)amino]-9,10-anthracenediones. *J. Med. Chem.* 1979; **22**: 1024–1030.
- Zee-Cheng R, Podrebarac E, Menon C, Cheng C. Structural modification study of bis(substituted aminoalkylamino)anthraquinones. An evaluation of the relationship of the [2-[(2-hydroxyethyl)amino]ethyl]amino side chain with antineoplastic activity. *J. Med. Chem.* 1979; **22**: 501–505.
- Kalopissis G, Bugaut A. Basic anthraquinone hair dye. *Chem. Abstr.* 1970; **73**: 59.
- Zagotto G, Mitaritonna G, Sissi C, Palumbo M. New peptidyl-anthraquinones: synthesis and DNA binding. *J. Med. Chem* 1996; **39**: 3114–3122.
- Morier-Teissier E, Boitte N, Helbecque N, Jean-Luc B, Pommery N, Duvalet J, Fournier C, Hecquet B, Catteau J, Henichart J. Synthesis and antitumour properties of an anthraquinone bisubstituted by the copper chelating peptide Gly-Gly-L-His. *J. Med. Chem.* 1993; **36**: 2084–2090.
- Cummings J, Macpherson J, Meikle I, Smyth J. Development of anthracenyl-amino acid conjugates as topoisomerase I and II inhibitors that circumvent drug resistance. *Biochem. Pharm.* 1996; **52**: 979–990.
- Meikle I, Cummings J, Macpherson J, Smyth J. Identification of anthracenyl-dipeptide conjugates as novel topoisomerase I and II inhibitors and their evaluation as potential anticancer drugs. *Anti-Cancer Drug Design* 1995; **10**: 515–527.
- Meikle I, Cummings J, Macpherson J, Hadfield J, Smyth J. Biochemistry of topoisomerase I and II inhibition by anthracenyl-amino acid conjugates. *Biochem. Pharm* 1995; **49**: 1747–1757.
- Greenhalgh C, Hughes N. The reaction of leucoquinizarins with alkylenediamines. *J. Chem. Soc (C)* 1968; 1284–1288.
- Bates A, Maxwell A. *DNA Topology*, Rickwood D (ed.). Oxford University Press: Oxford, 1993.
- Hertzberg R, Caranfa M, Hecht S. On the mechanism of topoisomerase I inhibition by camptothecin: evidence for binding to an enzyme-DNA complex. *Biochemistry* 1989; **28**: 4629–4638.
- Redinbo M, Stewart L, Kuhn P, Champoux J, Hol W. Crystal structure of human topoisomerase I in covalent and noncovalent complexes with DNA. *Science* 1998; **279**: 1504–1513.
- Fassberg J, Stella VJ. A kinetic and mechanistic study of the hydrolysis of camptothecin and some analogues. *J. Pharm. Sci.* 1992; **81**: 676–684.
- Denizli A, Piskin E. Dye-ligand affinity systems. *J. Biochem. Biophys. Methods* 2001; **49**: 391–416.
- Gaylord BS, Heeger AJ, Bazan GC. DNA detection using water-soluble conjugated polymers and peptide nucleic acid probes. *Proc. Natl Acad. Sci. USA* 2002; **99**: 10954–10957. Epub 2002 Aug 07.